Available online at www.sciencedirect.com
ScienceDirect
Solid State Sciences 10 (2008) 1773–1776
www.elsevier.com/locate/ssscie

Comparison among superconducting models for β″-$ET_4[(H_3O)Fe(C_2O_4)_3]\cdot C_6H_5Br$ single crystals by scanning tunnelling spectroscopy

A. Gambardella [a,*], R. Di Capua [a], M. Salluzzo [a], R. Vaglio [a], M. Affronte [b], U. del Pennino [b], S. Curreli [c], C. Giménez-Saiz [c], C.J. Gómez-García [c], E. Coronado [c]

[a] CNR-INFM/Coherentia, Complesso Monte S. Angelo, Via Cinthia, 80126 Napoli, Italy
[b] CNR-INFM S3 National Research Center and Dipartimento di Fisica, Università di Modena e Reggio Emilia, Via Campi 213a, 41100 Modena, Italy
[c] Instituto de Ciencia Molecular, Universitat de Valencia, Edif. Institutos 46980 Paterna Valencia, Spain

Received 26 October 2007; received in revised form 20 December 2007; accepted 21 December 2007
Available online 3 January 2008

Abstract

Single crystals of the novel superconductor β″-$(BEDT\text{-}TTF)_4[(H_3O)Fe(C_2O_4)_3]\cdot C_6H_5Br$ charge-transfer salt were studied using a scanning tunnelling microscope. The measured samples have an onset critical temperature of about 4.0 K. Features often reported on similar compounds were observed in the tunnelling spectra at 1.4 K. STS spectra are compared with several models for the superconducting density of states. Our analysis evidences inhomogeneous superconductivity and indicates that the presence of a magnetic layer into the sample plays a role in determining the superconducting spectroscopic features.

Keywords: Organic superconductors; Scanning tunnelling microscopy and spectroscopy; BEDT-TTF

1. Introduction

Superconducting derivatives of the BEDT-TTF (bis(ethylenedithio)-tetrathiafulvalene (or ET for short)) molecule have been extensively studied because of their unconventional properties [1]. Stable ionic crystalline lattices formed by alternate layers of cationic (donor) ET molecules and anionic (acceptor) molecules are currently synthesised in different packing motives. In such compounds the transport properties are influenced by the disorder associated with the configuration of the ethylene groups within the cation layer, which is overall crucial for stabilizing the superconducting state. Moreover, it has been suggested that the presence of magnetic ions could play some role in the superconducting state, especially in the suppression of the critical temperature (T_c) [2,3], as well as the intrinsic disorder can do [4]. Scanning tunnelling microscopy and spectroscopy (STM/STS) represent powerful techniques to provide information, on a local scale, about the role of intrinsic disorder and of magnetic layers on the superconducting properties of the ET derivatives. Here we report STM and STS investigations on a novel member of the family of β″-$ET_4[(H_3O)M(C_2O_4)_3]\cdot Y$ crystals, where M is a metal atom and Y is a guest molecule, with M = Fe and $Y = C_6H_5Br$.

2. Experimental procedure

Single crystals of β″-$ET_4[(H_3O)Fe(C_2O_4)_3]\cdot C_6H_5Br$ were grown by electrocrystallization techniques, as described elsewhere [5]; the crystals are typically prismatic rods, about $2 \times 1 \times 0.1\ mm^3$.

The crystal orientation was determined by X-ray diffraction measurements (details are given in Ref. [5]), and the reported resistivity vs. temperature curve was measured along the *a*–*b* plane. Nevertheless, the measured in-plane normal state

* Corresponding author.
E-mail address: gambardella@na.infn.it (A. Gambardella).

1293-2558/$ - see front matter © 2008 Elsevier Masson SAS. All rights reserved.
doi:10.1016/j.solidstatesciences.2007.12.033

conductivity is reproducibly smaller than what reported in earlier papers for analogous compounds (see for example Ref. [6]), and is more similar to the one along the *c* axis [6]. We attribute this result to the fact that in our crystals there is a large interlayer contribution due to the presence of dislocations, and the four-contact determination of the absolute value of the resistivity is affected by such contribution.

The crystals measured by STM have an onset $T_c \sim 4.0$ K (T_c at zero resistance ~ 0.5 K), as determined by resistivity vs. temperature measurement reported in Fig. 1.

Surface topography measurements were carried out by a home-made STM (in He atmosphere) and by a standard Omicron VT-STM (in Ultra High Vacuum). STS was performed with the home-made scanner in a cryogenic environment able to cool the sample down to 1.3 K. Samples were mounted on the scanner and sealed in inert He atmosphere to avoid condensation on the sample surface at low temperatures. We used PtIr tips, electrochemically etched. The differential tunnelling conductance d*I*/d*V* is obtained directly by a standard lock-in technique.

3. Tunnelling measurements

Fig. 2 shows a topographic image taken at room temperature. The surface appears granular, with a roughness of some nanometers (grain dimensions are about some tens of nanometer). Topography reveals sub-structured arrays (or stripes) constituted by packed foils (Fig. 2a and b) which reflect the layered structure of the crystal. These macrostructures are sometimes superimposed to twinning patterns (Fig. 2c) probably related to the crystal growth.

The tunnelling spectra in Fig. 3a were acquired at $T = 1.4$ K, stabilizing the junction at a bias voltage of 30 mV and a tunnel current of 100 pA. Spectra recorded in different locations sometimes show different qualitative features, indicating a non-homogenous surface superconductivity. It is hard to attribute the inhomogeneity to a specific reason, since many factors can contribute to it. Intrinsic differences in the local spectroscopic features (also due to the non-complete transition at $T = 1.4$ K) and extrinsic factors related to the granular surface can both concur. Furthermore, at present we cannot exclude to have contributions to the tunnelling current from different layers of the compound with position-dependent weights. The main qualitative features of the tunnelling spectra are however well clear and reproducible. The V-shaped or parabolic background, the relatively high energy (compared to $k_B T_c$) of the gap-like structures, and the absence of sharp peaks in these structures are common features in the organic superconducting compounds. Moreover, they resemble the spectra reported by many authors on the more studied κ-ET derivatives, such as the κ-$(ET)_2Cu(NCS)_2$ [7,8]. Such similarities seem to indicate that some general properties are common to the members of this class of compounds, as concerns, for instance, the role of intrinsic disorder in influencing the transport and the electronic features.

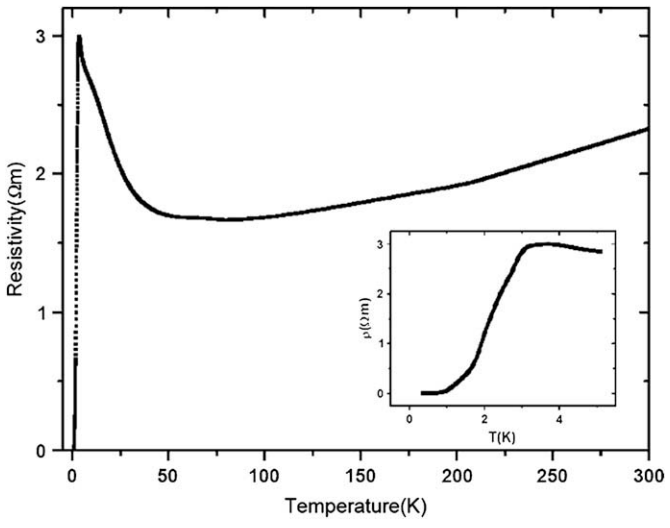

Fig. 1. In-plane resistivity vs. temperature curve for the measured β″-$ET_4[(H_3O)Fe(C_2O_4)_3]\cdot C_6H_5Br$ single crystals.

Most of the STM–STS works on ET derivatives were performed on higher T_c (around 10–14 K) compounds [7,8]. Comparing to these works, the higher zero bias tunnel conductance value measured on our samples can be ascribed to the lower T_c (and therefore to the higher T/T_c ratio) and to the presence of a stronger paramagnetic layer containing Fe, as discussed in the following.

Despite the lack of the coherence peaks, the relation between the observed spectroscopic features and the superconductivity is confirmed by the behaviour as a function of the temperature (Fig. 3b), which shows that the depletion of the density of states (DOS) around the Fermi level takes place below the onset T_c.

For a quantitative evaluation, a model for the DOS must be considered. The symmetry of the pair wave function is still an open issue. Knight shift measurements [9,10] and theoretical considerations on the Bethe–Salpeter equation [11] indicated that a singlet s- or d-wave state (even both in frequency and in momentum) should describe the pairing symmetry, but the experimental results [12–14] and their interpretation are still controversial on this point. Therefore which of the two models more suitable to these compounds is not yet clear. In Fig. 4a, the fit results with both models are shown on one of the STS recorded spectra. The experimental data have been normalized using a parabolic background. The fitting curves have been evaluated assuming for the DOS the following expression:

$$N(E) \propto \frac{1}{2\pi}\int_0^{2\pi}\left| Re\frac{E - i\Gamma}{\sqrt{(E - i\Gamma)^2 - \Delta(\theta)^2}}\right| d\theta \qquad (1)$$

where E is the energy ($E = 0$ being the Fermi level), Γ the Dynes broadening parameter [15], θ the azimuthal angle in the reciprocal space and $\Delta(\theta)$ the gap as a function of the **k**-vector. In the s-wave model, $\Delta(\theta) = \Delta_0$, constant, while in the simple $d_{x^2-y^2}$-wave model, $\Delta(\theta) = \Delta_0 \cos 2\theta$.

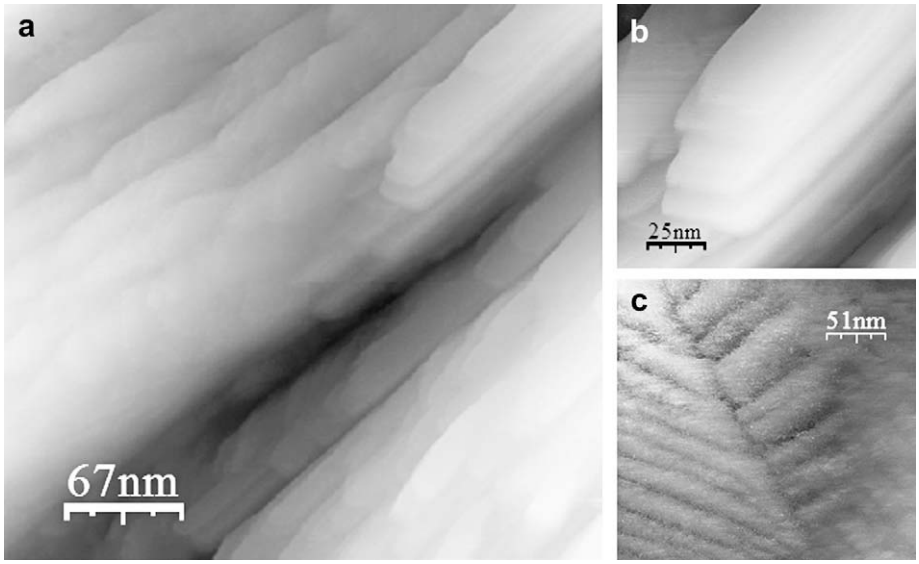

Fig. 2. Room temperature STM topographic images taken on an $ET_4[(H_3O)Fe(C_2O_4)_3]\cdot C_6H_5Br$ single crystal (bias voltage: 2 V; tunnel current: 10 pA). (a and b) Images show stepped stripes; (c) evidence for twinning planes.

The d-wave model reproduces the shape of the experimental STS near the Fermi level curve better than the s-wave one. For both fitting curves, the $2\Delta_0/k_BT_c$ ratio is greater than the BCS theoretical value 3.5:29 for the d-wave, 23 for the s-wave. These findings resemble what already reported on the κ-ET derivatives. We also consider an alternative point of view to evaluate the experimental data. The commonly used s-wave and d-wave models do not take into account the presence of paramagnetic planes in the crystal structure, the effect of impurities or scattering being represented only by the phenomenological Dynes broadening parameter Γ. In the measured crystals, the superconducting ET layers are alternated with paramagnetic [5] $(H_3O)^+[Fe(C_2O_4)_3]^{3-}$ layers. The behaviour of superconducting paramagnetic alloys was originally studied by Abrikosov and Gor'kov [16]. Using the many-body systems' techniques in the frame of the Abrikosov-Gor'kov (AG) theory, the effect of magnetic impurities on the energy spectrum can be evaluated and an appropriate expression for the DOS can be inferred. The main prediction is the rising of a gapless superconductivity when the paramagnetic concentration is high enough. An approximate expression for the DOS [17] in this case is given by

$$N(E) \propto 1 + \frac{1}{2}\frac{(E/\Delta)^2 - \alpha^2}{\left[(E/\Delta)^2 + \alpha^2\right]^2} \tag{2}$$

where Δ is the (temperature dependent) AG order parameter, which no longer represents an energy gap in the quasi-particle excitation spectrum; α is proportional to n_i/Δ, n_i being the concentration of paramagnetic impurities. In Fig. 4b, the best result obtained with the above formula is shown. Compared with the above-mentioned models, the AG DOS is able to qualitatively describe the absence of sharp coherence

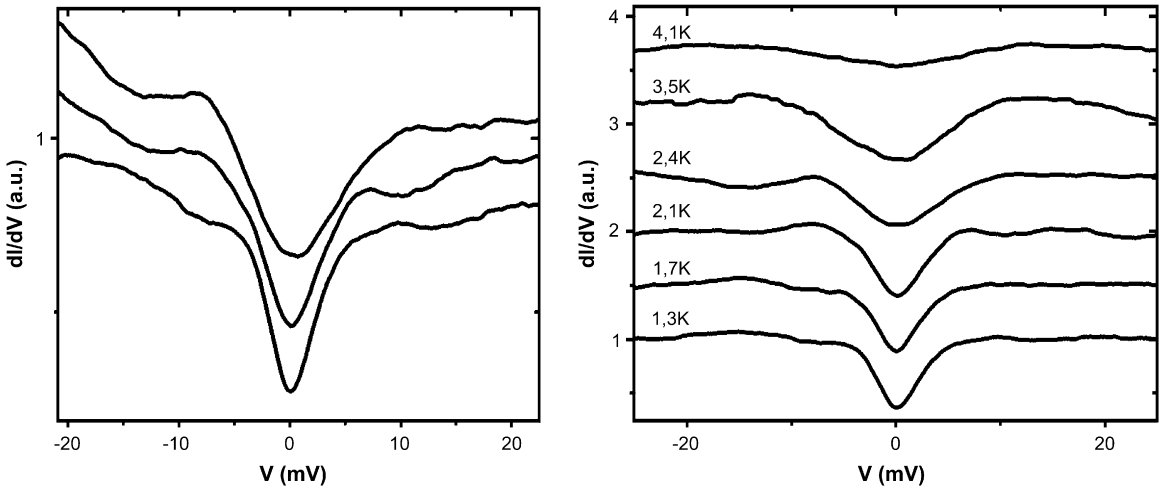

Fig. 3. (a) Typical STS spectra recorded on $ET_4[(H_3O)Fe(C_2O_4)_3]\cdot C_6H_5Br$ single crystals at different surface locations (raw data); (b) temperature dependence of STS spectra in a fixed position; the curves are shifted for clarity.

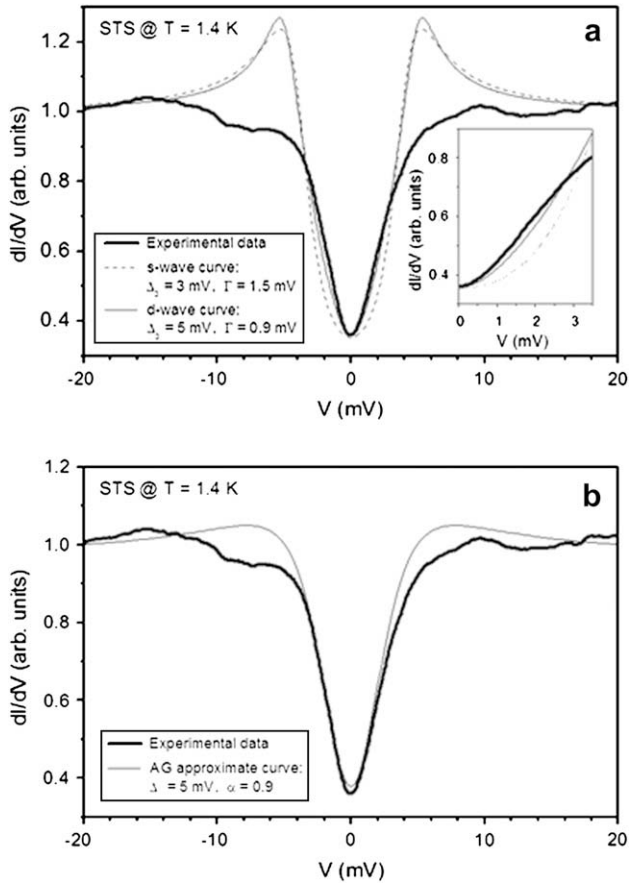

Fig. 4. STS theoretical curves by several models are superimposed to the experimental data. (a) s-Wave and d-wave BCS-like models; the inset shows a magnification of the intra-gap region; (b) AG approximated model.

peaks. It must be remarked that Eq. (2) is an approximation to the theoretical DOS in the presence of paramagnetic impurities. Strictly speaking, it is reliable for $\alpha > 1$ (gapless condition), which is not the case of the curve in Fig. 4b. Furthermore, the crystals can be seen as an intrinsically disordered system near the metal–insulator transition. In an unconventional framework, disorder, even non-magnetic, might act as strong scattering centres, causing a suppression of superconductivity and then explaining the smearing of the DOS (again in AG-like scenario), similarly to what happens in s-wave superconductor where magnetic impurities cause the suppression of T_c. However, we would like to emphasize two points. First, even in the approximated form given by Eq. (2), the AG model provides a better description of the tunnel spectra on our crystal and in general on the organic superconducting compounds of this family (as remarked above, the measured features are common to such compounds), compared with the simple s- and d-wave BCS DOSs. Second, better fitting, with higher α values, can be obtained through Eq. (2) on the spectra which exhibit a more depressed superconductivity; this circumstance is a strong indication that the different weight, as a function of the surface position, of the paramagnetic layers on the tunnel current plays a major role in determining the inhomogeneities in the STS spectra.

4. Conclusions

STS measurements on β''-$ET_4[(H_3O)Fe(C_2O_4)_3]\cdot C_6H_5Br$ superconducting crystals were performed by a cryogenic STM. The tunnelling spectra below the transition temperature can be fitted, in the low energy (sub-gap) range with a d-wave model for the DOS, which reproduce the shape of the d*I*/d*V* vs. *V* curve better than the conventional s-wave DOS. However, an even better overall fit is provided by considering the role of the paramagnetic $(H_3O)^+[Fe(C_2O_4)^3]^{3-}$ layers. The consequent ''smoothed'' DOS, even in an approximated form, can indeed reproduce the whole tunnelling spectrum. This analysis suggests that the magnetic layers and ions included in the crystal structure could have a fundamental role in determining the superconducting properties of the investigated compound, and possibly those of the compounds of the same family which exhibit magnetic behaviour close to the superconducting state in the phase diagram (as already indicated by some considerations on the results from different techniques [18]). The topographic STM image in Fig. 2 has been processed by using the WSxM software, developed by Horcas et al. [19].

References

[1] F. Kagawa, K. Miyagawa, K. Kanoda, Nat. Lett. 436 (2005) 534.
[2] L. Balicas, J.S. Brooks, K. Storr, S. Uji, M. Tokumoto, H. Tanaka, H. Kobayashi, A. Kobayashi, V. Barzykin, L.P. Gorkov, Phys. Rev. Lett. 87 (2001) 067002.
[3] O. Cepas, R.H. McKenzie, J. Merino, Phys. Rev. B 65 (2002) 100502.
[4] A.I. Coldea, A.F. Bangura, J. Singleton, A. Ardavan, A. Akutsu-Sato, H. Akutsu, S.S. Turner, P. Day, Phys. Rev. B 69 (2004) 085112.
[5] E. Coronado, S. Curreli, C.C. Giménez-Saiz, C.J. Gòmez-Garcìa, J. Mater. Chem. 15 (2005) 1429.
[6] H. Akutsu, A. Akutsu-Sato, S.S. Turner, D. Le Pevelen, P. Day, V. Laukhin, A.-K. Klehe, J. Singleton, D.A. Tocher, M.R. Probert, J.A.K. Howard, J. Am. Chem. Soc. 124 (2002) 12430.
[7] T. Arai, K. Ichimura, K. Nomura, S. Taksaki, J. Yamada, S. Nakatsuji, H. Anzai, Phys. Rev. B 63 (2001) 104518.
[8] K. Ichimura, S. Higashi, K. Nomura, A. Kawamoto, Synth. Met. 153 (2005) 409.
[9] S.M. De Soto, C.P. Slichter, A.M. Kini, H.H. Wang, U. Geiser, J.M. Williams, Phys. Rev. B 52 (1995) 10364.
[10] H. Mayaffre, P. Wzietek, D. Jérome, C. Lenoir, P. Batail, Phys. Rev. Lett. 75 (1995) 4122.
[11] M. Vojta, E. Dagotto, Phys. Rev. B 59 (1999) R713.
[12] A. Carrington, I.J. Bonalde, R. Prozorov, R.W. Giannetta, A.M. Kini, J. Schlueter, H.H. Wang, U. Geiser, J.M. Williams, Phys. Rev. Lett. 83 (1999) 4172.
[13] M. Pinteric, S. Tomic, M. Prester, D. Drobac, O. Milat, K. Maki, D. Schweitzer, I. Heinen, W. Strunz, Phys. Rev. B 61 (2000) 7033.
[14] H. Elsinger, J. Wosnitza, S. Wanka, J. Hagel, D. Schweitzer, W. Strunz, Phys. Rev. Lett. 84 (2000) 6098.
[15] R.C. Dynes, V. Narayanamurti, J.P. Garno, Phys. Rev. Lett. 41 (1978) 1509.
[16] A.A. Abrikosov, L.P. Gor'kov, Sov. Phys. JETP 12 (1961) 1243.
[17] V. Ambegaokar, A. Griffin, Phys. Rev. 137 (1965) A1151.
[18] B.J. Powell, R.H. McKenzie, Phys. Rev. B 69 (2004) 024519.
[19] I. Horcas, R. Fernández, J.M. Gómez-Rodriguez, J. Colchero, J. Gómez-Herrero, A.M. Baro, Rev. Sci. Instrum. 78 (2007) 013705.